

Characterization of Carbons Produced from Gelidium Corneum and Adsorption of Crystal Violet

Mikhail OLAM*

Department of Chemical Engineering, Inonu University, Malatya, 44280, Turkey

<http://doi.org/10.5755/j02.ms.36875>

Received 4 April 2024; accepted 10 June 2024

Due to high production costs, the production of activated carbon from waste has attracted a lot of attention recently. In this study, gelidium corneum (GC) was carbonized at 800 °C for 90 min. Its carbonization yield, adsorption capacity, and physical and chemical properties were investigated. Ultraviolet-visible spectroscopy (UV), X-ray diffraction (XRD), Fourier-transform infrared spectroscopy (FTIR), energy-dispersive X-ray spectroscopy (EDX), scanning electron microscopy (SEM), proximate analysis and ultimate analysis were performed. According to XRD analysis, the structure of GC is semi-crystalline, but the crystalline structure increases after carbonization. The carbonization yield of GC was about 39%. According to SEM, UV and XRD analysis, the carbonization process supported crystallinity and the formation of micropore/mesopore structures. The crystal violet (CV) removal and adsorption capacity were 96 % and 9.63 mg/g at an initial dye concentration of 50 mg/L, 30 °C, adsorbent dosage of 5 g/L, constant stirring speed of 200 rpm and equilibration time of 60 min, respectively. The carbonized gelidium corneum (cGC) can be used as a suitable adsorbent for the removal of dyes from aqueous solutions. It can also be an alternative product to commercial products because of its high adsorption capacity and cost-effectiveness.

Keywords: gelidium corneum, activated carbon, adsorption, crystal violet.

1. INTRODUCTION

Industrial wastes contain significant concentrations of dye [1]. Many methods, including chemical reduction, electrochemical purification, evaporation, chemical precipitation and adsorption, reverse osmosis, filtration, and ion exchange, are used to remove water contaminants [2–4]. Most of these are generally limited in their use due to their high cost, energy consumption, and the generation of large amounts of toxic waste [5]. However, activated carbons produced from bio-based wastes eliminate some of these disadvantages. Activated carbons, produced from many sources such as biomass and waste plastics, have a high surface area [6, 7]. Therefore, they are widely used in many applications such as separation/purification of gases and liquids, production of composite materials, catalyst/catalyst support, removal of toxic substances, supercapacitors, and electrodes [8–13]. The physical/chemical activation processes are generally applied to increase the surface area and surface activity of activated carbons [14]. After the carbonization process, numerous micropores, mesopores, and macropores are formed within their structures [15, 16]. If the physical/chemical activation is not done before/after carbonization, micropores may not form significantly [17, 18]. While the adsorption capacity of the carbons obtained from waste onions is 8.7 mg/g, the adsorption capacity of their activation with KOH is 18.6 mg/g [19]. Dil et al. [20] found that the CV dye adsorption of a commercial activated carbon was 35 mg/g, while zinc (II) oxide nanorod loaded on activated carbon (ZnO-NRs-AC) was 81 mg/g. Guo et al. suggested that sulfuric acid (H₂SO₄)-activated

carbons are more effective than CO₂-activated carbons for removing ammonia (NH₃). However, this improvement is not solely dependent on their surface area [21]. On the other hand, these processes could seriously increase production costs [22]. To produce an economical adsorbent, cost-increasing additional processes should be avoided as much as possible. Therefore, in this study, waste biomass (gelidium corneum) was carbonized directly (only dried in the sun) without washing or drying, and no chemical or physical activation process was applied. The effect of the carbons on the removal of crystal violet (CV) from wastewater was then determined. Gelidium corneum (GC) is a well-known red seaweed that grows on sea coasts [23]. Many commercial products, such as agar, are derived from gelidium and are utilized in various industries, particularly in cosmetics and food [24, 25]. However, there are no available studies on the removal of CV from carbonized gelidium corneum (cGC). This study examined the physical and chemical properties of cGC and its potential for removing CV dye.

CV is a cationic dye widely used in the industry [26]. Cationic dyes may easily interact with cell membrane surfaces and may also concentrate in the cytoplasm inside the cell, making them more harmful than anionic dyes [27, 28]. Additionally, CV is widely used in applications such as medicinal solutions and animal feeds [29]. However, these applications result in the generation of dye effluent, which is discharged into the sea and lakes through the sewage system. CV is considered harmful to biological life as it is a strong carcinogen and promotes tumor growth [30, 31]. Therefore, the removal of CV from wastewater is crucial for the environment and biological life.

* Corresponding author. Tel.: +905327634534.
E-mail: mikhail.olam@inonu.edu.tr (M. Olam)

2. MATERIAL AND METHOD

2.1. Material

In experimental studies, CV (Carlo Erba, purity: 99 %, C.I.:42555, Cas No: 548-62-9), whose molecular weight is 407.98 g/mol and empirical formula is $C_{25}H_{30}N_3Cl$ [32], was used as adsorbate. CV solution was prepared by dissolving it in 1000 mg/L of distilled water. GC gathered on the shores of the Marmara Sea in Istanbul, Turkey. GC contains moisture of 6.0 %, ash of 22.4 %, volatile matter of 68.3 %, and fixed carbon of 3.3 % (Table 1). As seen in the ultimate analysis of GC in Table 1, it contains carbon (C) of 26.6 %, hydrogen (H) of 4.5 %, oxygen (O) of 62.1 %, nitrogen (N) of 2.6 %, and sulphur (S) of 4.2 %. The carbon content in the material is low but still higher than most biomass [33]. In addition, Fig. 1 shows the results of the EDX analyses performed on the 10 μm surfaces of the samples.

The GC samples also contain calcium (Ca), potassium (K), silicon (Si), aluminum (Al), magnesium (Mg), phosphorus (P), chlorine (Cl), and sodium (Na).

Table 1. Ultimate and proximate analysis

Proximate analysis, wt.%		Ultimate analysis, wt.%, daf		Carbonization yield, %
Moisture	6.0	Carbon (C)	26.6	
Ash	22.4	Hydrogen (H)	4.5	
Volatile matter	68.3	Nitrogen (N)	2.6	
Fixed carbon*	3.3	Sulfur (S)	4.2	
		Oxygen (O*)	62.1	

*Calculated by difference

2.2. Methods

2.2.1. Analysis

The microstructure of the natural gelidium corneum (GC) and the carbonized gelidium corneum (cGC) were examined by scanning electron microscopy (SEM, LEO EVO 40). The quantitative determinations of GC and the cGC were made with PerkinElmer Spectrum One FTIR (650–4000 cm^{-1} , 2 cm^{-1} resolution and 128 scanning). Adsorption experiments were implemented with a UV-visible spectrophotometer (Shimadzu UV-1700 Pharmaspec) at 590 nm.

2.2.2. Experiments

The experimental procedure is given in Fig. 2.

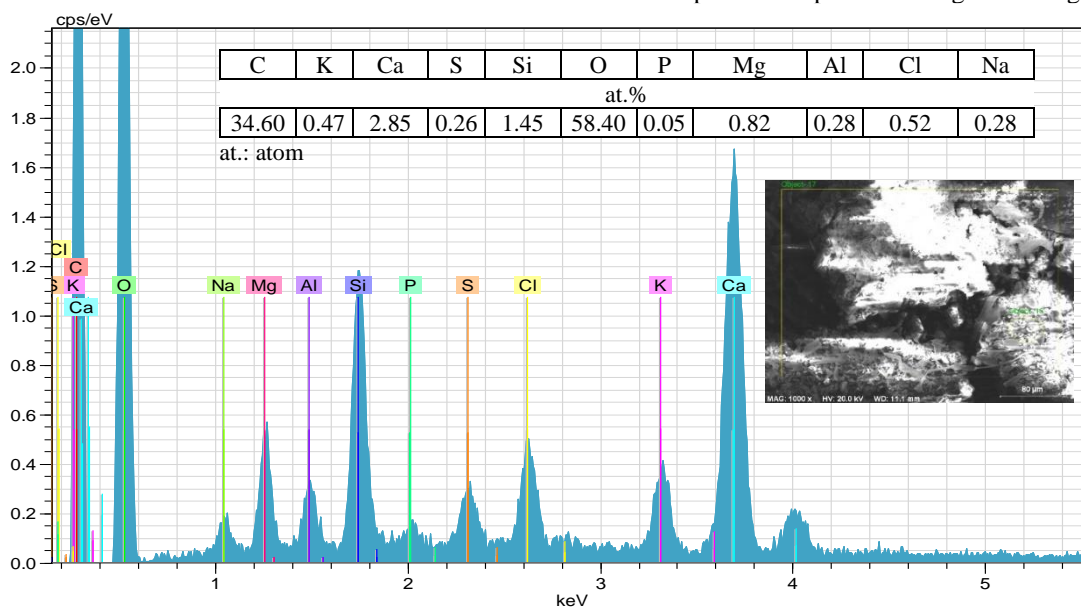


Fig. 1. EDX spectrum of GC

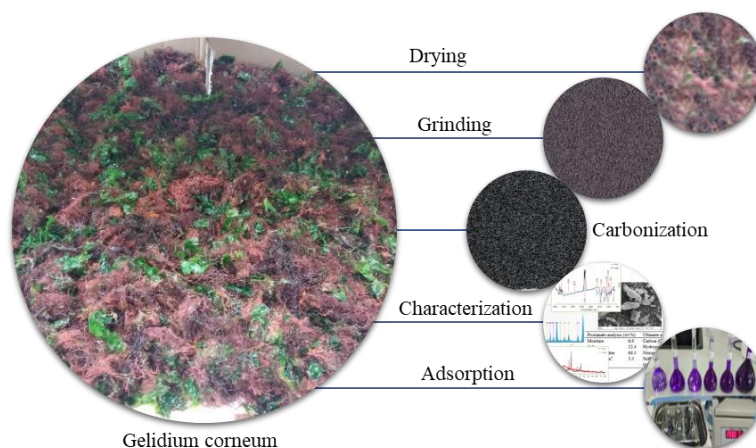


Fig. 2. Experimental procedure

The equilibrium adsorption, q_e (mg/g), was calculated using Eq. 1, and the percentage of CV removal (%) was determined using Eq. 2.

$$q_e = \frac{C_i - C_e}{m} \cdot V; \quad (1)$$

$$\text{Removal (\%)} = \frac{C_i - C_e}{C_i} \cdot 100, \quad (2)$$

where, q_e (mg/g) represents the amount of dye adsorbed per unit mass of the cGC. C_i (mg/L) is the initial dye concentration of CV, and C_e (mg/L) is the equilibrium adsorption of CV, and m (g) stands for the amount of the cGC, and V (L) represents the volume of the solution.

The carbonization yield of GC (Gy) was calculated according to Eq. 3.

$$\text{Gy (\%)} = \frac{W_a}{W_b} \times 100, \quad (3)$$

where, W_b (g) is the dry weight of GC, and W_a (g) is the weight of carbonized GC.

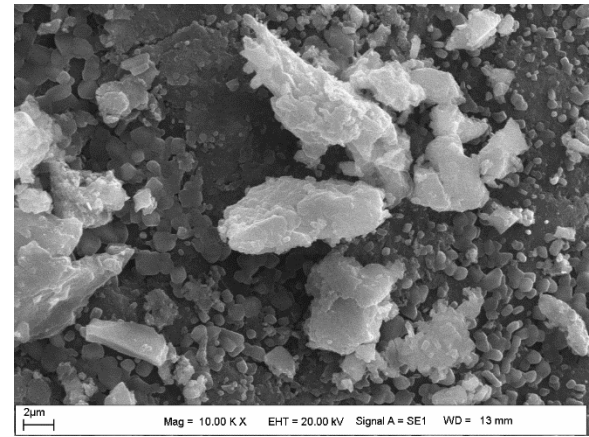
3. RESULTS AND DISCUSSION

3.1. Characterization of adsorbent

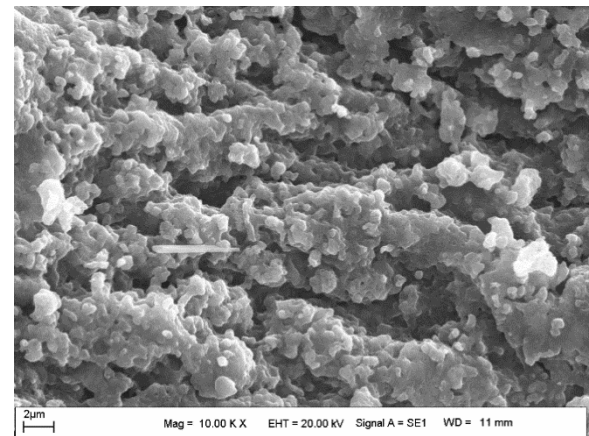
The carbonization yield of GC was 38.60 % under these conditions (Table 1). Duckweed's carbonization yield is 34 % [32]. Slash pine wood's carbonization yield is 28 % [34]. The carbonization yield of rice husk chemically activated with sulfuric acid (H_2SO_4) and zinc chloride ($ZnCl_2$) is 36 % and 32 %, respectively [35]. In summary, it can be said that the carbonization yield of GC is satisfactory.

The structure of GC and the cGC were analyzed by SEM (LEO-EVO 40). SEM analyses of GC before and after carbonization are given in Fig. 3. As seen in Fig. 3 a, there were no porous structures in the surface morphology of GC before carbonization, while porous structures were observed after carbonization (Fig. 3 b). SEM micrograph of the cGC showed the presence of pores of different sizes, indicating that very rough and heterogeneous textures were formed. This is highly beneficial as it provides greater surface availability for adsorption, thus increasing the adsorption efficiency of CV [36, 37]. Fourier transform infrared (FTIR), which is used as a qualitative technique [38], was applied to determine the functional groups on the surface of gelidium corneum (GC) before and after carbonization. As seen in the FTIR spectrum of GC given in Fig. 4, O-H stretching at 3265 cm^{-1} [39], C-H stretching at 2927 cm^{-1} [40, 41], C-H bending at 856 cm^{-1} [42], C=C stretching at 1635 cm^{-1} [43], C-C stretching at 1436 cm^{-1} [44], C-OH stretching at 1019 cm^{-1} [45], and C-O-C symmetrical stretching at 1229 cm^{-1} occurred [46]. Most of these bands disappeared after carbonization (cGC). This may have been caused by the high carbon content of the cGC.

As the ratio of elements such as hydrogen (H) and oxygen (O) in a substance decreases, their bands in the FTIR spectrum disappear [47]. After carbonization of the cGC, many of these peaks disappeared, and the hydroxyl group peak of 3286 cm^{-1} shifted to 3773 and 3656 cm^{-1} , and the C-O stretching peak of 1019 cm^{-1} shifted to 1107 cm^{-1} , and the C-O stretching peak of 1436 cm^{-1} shifted to 1430 cm^{-1} , and the $C\equiv C$ stretching band of 2347 cm^{-1} appeared.



a



b

Fig. 3. SEM image of GC: a – before carbonization; b – after carbonization

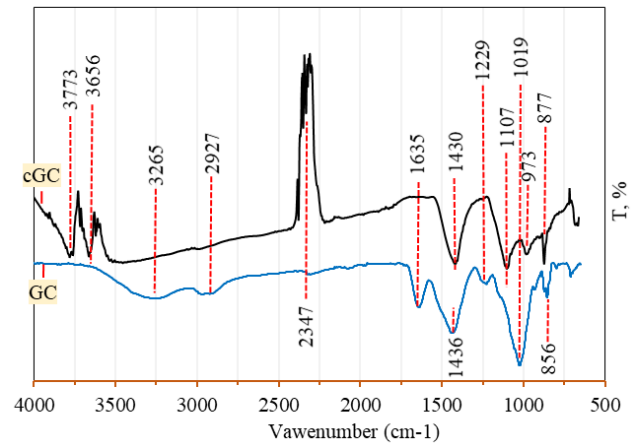


Fig. 4. FTIR analysis

The cGC appeared the strong bands at 2347 cm^{-1} ($C\equiv C$ stretch) and 1107 cm^{-1} (C-O stretch), and weak bands at 3780 and 3652 cm^{-1} (O-H stretch). The cGC showed the presence of many functional groups, binding sites responsible for CV absorption.

The prediction of the adsorption mechanism of CV dye on the cGC surface is shown in Fig. 5. The positively charged groups of CV and the negatively charged groups of the cGC surface may contribute to the electrostatic forces [48].

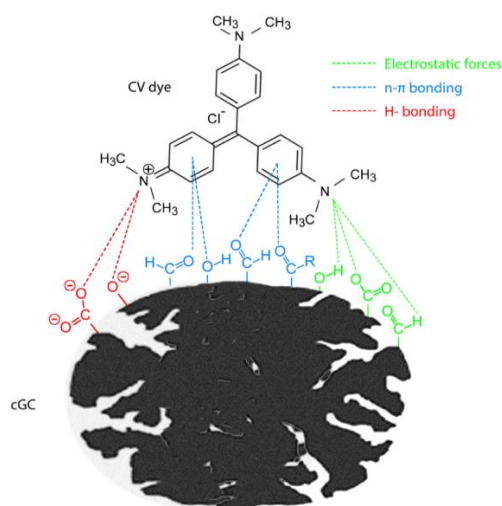


Fig. 5. Illustration of the possible interaction between the cGC surface and CV (H-bonding, n- π stacking, and electrostatic forces)

H-bonding may occur between the hydrogen on the surface of the cGC and the nitrogen atoms in the structure of the CV dye [49]. The n- π interaction may have played a role in CV adsorption through the interaction between the cGC surface and CV aromatic rings [50].

The physical properties, chemical composition and crystallographic structure of GC and the cGC were investigated by X-ray diffraction (XRD) analysis (Fig. 6). As can be seen in Fig. 6, in the XRD analysis of GC, a broad diffraction peak occurred around $2\theta = \sim 22^\circ$, corresponding to the diffraction of the (002) planes, which corresponds to the typical graphite plane [51].

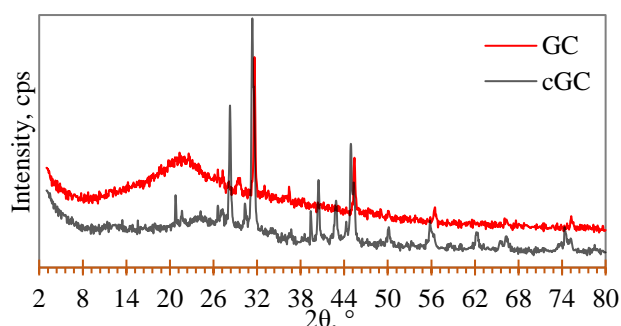


Fig. 6. XRD patterns of GC and cGC

Table 2. Removal of CV

Sample name	Chemical/physical treatment	Adsorbent dosage, g/L	Initial concentration, mg/L	Removal, %	q_e , mg/g	
cWC (Carbonized waste coffee)	none	5	50	25	2.52	[62]
cDW (Carbonized duckweed)	none	5	50	96	9.62	[32]
Activated carbon lemon wood/ Fe_3O_4	commercial	5	10	99	~2	[63]
Functionalized multi-walled carbon nanotubes (fMWNTs)	commercial	0.5	50	82	90	[64]
NaOH-activated aerva javanica leaf (NAJL)	NaOH	0.4	50	98	3.7	[65]
PLAC (Poultry litter activated carbon)	ZnCl_2	2.5	50	92	70.3	[66]
cLM/HS (Carbonized hazelnut shell and lemna minor)	none	1	100	88	87.95	[67]
Fe_3O_4 -MNPs (Magnetic nanoparticles modified with $\text{NaC}_{12}\text{H}_{25}\text{SO}_4$)	NaOH	0.25	10	80	166.67	[68]
cGC	none	5	50	96	9.63	This study

The broadening of the peak indicates the presence of amorphous carbon and a low degree of graphitization [52]. In addition, distinctive diffraction peaks occurred at 31° , 45° , 56° and 75° . This may have been caused by the presence of many elements (C, O, H, K, Ca, S, Si, P, Mg, Al, Cl, Na) in the content of GC (Fig. 1). It can be said that GC has a semi-crystalline structure due to the formation of a wide diffraction peak at about 22° , and prominent peaks at 31° , 45° , 56° and 75° . However, carbonization of GC (cGC) at 800°C , $2\theta = 22^\circ$ wide diffraction peaks almost disappeared, and 20° , 26° , 28° , 30° , 31° , 39° , 40° , 42° , 44° , 45° , 50° , 55° , 62° and 74° diffraction peaks occurred. In XRD phase analysis, it was indexed to correspond to sylvite (KCl) at 28° and 40° [53], and calcium sulfide (CaS) at 31° , 44° , 55° and 74° [54], and silicon tetrachloride (SiCl_4) at 45° and 50° [55], and silica (SiO_2) at 20° , 26° , 30° , 39° , 42° [56, 57], and magnesium oxide (MgO) at 62° [58]. The presence of these elements was supported by EDX analysis (Fig. 1). This shows that the graphite structure is destroyed and porous structures are formed [59], which is quite compatible with the SEM image given in Fig. 3.

3.2. Adsorption capacity of adsorbent

CV dye removal of carbonized GC (cGC) and the results obtained in current studies are given in Table 2. Adsorption experiments were carried out under specified conditions, which were 30°C , pH:6, adsorbent dosage of 5 g/L, contact time of 60 min, and initial concentration of 50 mg/L. The removal (%) and adsorption capacity were 96 % and 9.63 mg/L, respectively. Activated with NaOH, the NAJL achieved 98 % removal with the adsorbent dosage of 0.4 g/L, while the cGC was 96 % at the adsorbent dosage of 5 g/L (Table 2). Chemical and physical activation can improve the pore structure and surface areas of carbons, although they increase the cost of adsorbent production [60, 61]. The cGC provided more CV removal than the cWC. The activated carbon lemon wood/ Fe_3O_4 provides 98 % removal at the initial concentration of 10 mg/L, while the cGC can reach at higher (50 mg/L) initial concentrations. Compared to the existing adsorbents used in CV removal given in Table 2, it can be said that the adsorption capacity of the cGC is satisfactory.

The adsorption capacity of the cGC can be further increased by determining adsorption parameters such as absorbent dose, initial dye concentration, contact time, pH, and temperature.

4. CONCLUSIONS AND SUGGESTIONS

In this study, gelidium corneum (GC) carbonized at 800 °C for 90 min was characterized and its effectiveness was determined by the removal of crystal violet (CV) found in industrial wastewater. The obtained results are provided below.

1. Proximate analysis shows that the GC contains 22.4 % ash, 6.0 % moisture, 3.3 % fixed carbon, and 68.3 % volatile matter.
2. Ultimate analysis indicates that GC consists of 26.6 % C, 4.5 % H, 2.6 % N, 4.2 % S, and 62.1 % O.
3. According to EDX analysis, GC contains various elements such as C, K, Ca, S, Si, O, P, Mg, Al, Cl, and Na.
4. The carbonization yield of GC is 38.60 %.
5. FTIR analysis shows that the peaks of the functional groups of GC changed after carbonization.
6. SEM analysis reveals the formation of numerous porous structures after carbonization.
7. According to XRD analysis, the semi-crystalline structure of GC changed significantly to the crystalline structure after carbonization.
8. The cGC absorbent demonstrated a 96 % removal rate and an adsorption capacity of 9.63 mg/L for CV dye.

The cGC absorbent was proven to be both effective and inexpensive in the removal of CV dye from wastewater. Further research is needed to determine the optimal adsorption parameters for the cGC absorbent in CV removal.

Acknowledgments

The authors are thankful to Inonu University, Department of Chemistry and Mining Engineering, where the experimental studies were carried out.

REFERENCES

1. **Panahian, Y., Arsalani, N., Nasiri, R.** Enhanced Photo and Sono-photo Degradation of Crystal Violet Dye in Aqueous Solution by 3D Flower Like F-TiO₂(B)/fullerene Under Visible Light *Journal of Photochemistry and Photobiology A: Chemistry* 365 2018: pp. 45–51. <https://doi.org/10.1016/j.jphotochem.2018.07.035>
2. **Volesky, B.** Detoxification of Metal-Bearing Effluents: Biosorption for the Next Century *Hydrometallurgy* 59 (2–3) 2001: pp. 203–216. [https://doi.org/10.1016/S0304-386X\(00\)00160-2](https://doi.org/10.1016/S0304-386X(00)00160-2)
3. **Beigi, N., Shayesteh, H., Javanshir, S., Hosseinzadeh, M.** Pyrolyzed Magnetic NiO/Carbon-derived Nanocomposite from a Hierarchical Nickel-based Metal-organic Framework with Ultrahigh Adsorption Capacity *Environmental Research* 231 2023: pp. 116146. <https://doi.org/10.1016/j.envres.2023.116146>
4. **Arsalani, N., Nasiri, R., Zarei, M.** Synthesis of Magnetic 3D Graphene Decorated with CaCO₃ for Anionic Azo Dye Removal from Aqueous Solution: Kinetic and RSM Modeling Approach *Chemical Engineering Research and Design* 136 2018: pp. 795–805. <https://doi.org/10.1016/j.cherd.2018.06.024>
5. **El-Ahmady Ali El-Naggar, N., Hamouda, R.A., El-Khateeb, A.Y., Rabei, N.H.** Biosorption of Cationic Hg²⁺ and Remazol brilliant blue anionic dye from binary Solution Using Gelidium Corneum Biomass *Scientific Reports* 11 (1) 2021: pp. 1–24. <https://doi.org/10.1038/s41598-021-00158-0>
6. **Yang, K., Peng, J., Srinivasakannan, C., Zhang, L., Xia, H., Duan, X.** Preparation of High Surface Area Activated Carbon from Coconut Shells Using Microwave Heating *Bioresource Technology* 101 (15) 2010: pp. 6163–6169. <https://doi.org/10.1016/J.BIORTECH.2010.03.001>
7. **Olam, M.** Production of Activated Carbon from Waste PET' Chars *International Journal of Environmental Monitoring and Analysis* 10 (2) 2022: pp. 39. <https://doi.org/10.11648/j.ijema.20221002.13>
8. **Oda, H., Nakagawa, Y.** Removal of Ionic Substances from Dilute Solution Using Activated Carbon Electrodes *Carbon* 41 (5) 2003: pp. 1037–1047. [https://doi.org/10.1016/S0008-6223\(03\)00013-7](https://doi.org/10.1016/S0008-6223(03)00013-7)
9. **Yuan, A., Zhang, Q.** A Novel Hybrid Manganese Dioxide/activated Carbon Supercapacitor Using Lithium Hydroxide Electrolyte *Electrochemistry Communications* 8 (7) 2006: pp. 1173–1178. <https://doi.org/10.1016/J.ELECOM.2006.05.018>
10. **Fuente, A.M., Pulgar, G., González, F., Pesquera, C., Blanco, C.** Activated Carbon Supported Pt Catalysts: Effect of Support Texture and Metal Precursor on activity of Acetone Hydrogenation *Applied Catalysis A: General* 208 (1–2) 2001: pp. 35–46. [https://doi.org/10.1016/S0926-860X\(00\)00699-2](https://doi.org/10.1016/S0926-860X(00)00699-2)
11. **Moon, S.H., Shim, J.W.** A Novel Process for CO₂/CH₄ Gas Separation on Activated Carbon Fibers – Electric Swing Adsorption *Journal of Colloid and Interface Science* 298 (2) 2006: pp. 523–528. <https://doi.org/10.1016/J.JCIS.2005.12.052>
12. **Yıldırım GM, Bayrak B.** The Synthesis of Biochar-Supported Nano Zero-Valent Iron Composite and Its Adsorption Performance in Removal of Malachite Green *Biomass Conversion and Biorefinery* 12 (10) 2022: pp. 4785–4797. <https://doi.org/10.1007/S13399-021-01501-1>
13. **Shayesteh, H., Rahbar-Kelishami, A., Norouzbeigi, R.** Adsorption of Malachite Green and Crystal Violet Cationic Dyes from Aqueous Solution Using Pumice Stone as A Low-Cost Adsorbent: Kinetic, Equilibrium, and Thermodynamic Studies *Desalination and Water Treatment* 57 (27) 2016: pp. 12822–12831. <https://doi.org/10.1080/19443994.2015.1054315>
14. **Maciá-Agulló, J.A., Moore, B.C., Cazorla-Amorós, D., Linares-Solano, A.** Activation of Coal Tar Pitch Carbon Fibres: Physical Activation vs. Chemical Activation *Carbon* 42 (7) 2004: pp. 1367–1370. <https://doi.org/10.1016/J.CARBON.2004.01.013>
15. **Khamkeaw, A., Asavamongkolkul, T., Perngyai, T., Jongsomjit, B., Phisalaphong, M.** Interconnected Micro, Meso, and Macro Porous Activated Carbon from Bacterial Nanocellulose for Superior Adsorption Properties and Effective Catalytic Performance *Molecules* 25 (18) 2020: pp. 4063. <https://doi.org/10.3390/MOLECULES25184063>
16. **Hu, Z., Srinivasan, M.P.** Mesoporous High-surface-area Activated Carbon *Microporous and Mesoporous Materials*

- 43 (3) 2001: pp. 267–275.
[https://doi.org/10.1016/S1387-1811\(00\)00355-3](https://doi.org/10.1016/S1387-1811(00)00355-3)
17. **Caturla, F., Molina-Sabio, M., Rodríguez-Reinoso, F.** Preparation of Activated Carbon by Chemical Activation with ZnCl₂ *Carbon* 29 (7) 1991: pp. 999–1007.
[https://doi.org/10.1016/0008-6223\(91\)90179-M](https://doi.org/10.1016/0008-6223(91)90179-M)
 18. **Paraskeva, P., Kalderis, D., Diamadopoulos, E.** Production of Activated Carbon from Agricultural by-products *Journal of Chemical Technology & Biotechnology* 83 (5) 2008: pp. 581–592.
<https://doi.org/10.1002/JCTB.1847>
 19. **Bibi, F., Sattar, A., Hussain, S., Waseem, M.** Tailoring the Sorption Properties of Crystal Violet by Activated Carbon Extracted from Waste Onion *Chemical Papers* 77 (7) 2023: pp. 3957–3966.
<https://doi.org/10.1007/s11696-023-02756-w>
 20. **Dil, E.A., Ghaedi, M., Asfaram, A.** The Performance of Nanorods Material as Adsorbent for Removal of Azo Dyes and Heavy Metal Ions: Application of Ultrasound Wave, Optimization and Modeling *Ultrasonics Sonochemistry* 34 2017: pp. 792–802.
<https://doi.org/10.1016/j.ultsonch.2016.07.015>
 21. **Guo, J., Xu, W.S., Chen, Y.L., Lua, A.C.** Adsorption of NH₃ onto Activated Carbon Prepared from Palm Shells Impregnated with H₂SO₄ *Journal of Colloid and Interface Science* 281 (2) 2005: pp. 285–290.
<https://doi.org/10.1016/j.jcis.2004.08.101>
 22. **Lima, I.M., McAloon, A., Boateng, A.A.** Activated Carbon from Broiler Litter: Process Description and Cost of Production *Biomass and Bioenergy* 32 (6) 2008: pp. 568–572.
<https://doi.org/10.1016/j.biombioe.2007.11.008>
 23. **Mouga, T., Fernandes, I.B.** The Red Seaweed Giant Gelidium (*Gelidium corneum*) for New Bio-Based Materials in a Circular Economy Framework *Earth (Switzerland)* 3 (3) 2022: pp. 788–813.
<https://doi.org/10.3390/EARTH3030045/S1>
 24. **Lebbar, S., Fanuel, M., Le Gall, S., Falourd, X., Ropartz, D., Bressollier, P., Gloaguen, V., Faugeton-Girard, C.** Agar Extraction by-products from Gelidium Sesquipedale as a Source of Glycerol-galactosides *Molecules* 23 (12) 2018: pp. 3364.
<https://doi.org/10.3390/molecules23123364>
 25. **Cotas, J., Leandro, A., Pacheco, D., Gonçalves, A.M.M., Pereira, L.** A Comprehensive Review of the Nutraceutical and Therapeutic Applications of Red Seaweeds (Rhodophyta) *Life* 10 (3) 2020: p. 19.
<https://doi.org/10.3390/life10030019>
 26. **Nandi, B.K., Goswami, A., Das, A.K., Mondal, B., Purkait, M.K.** Kinetic and Equilibrium Studies on the Adsorption of Crystal Violet Dye Using Kaolin as an Adsorbent *Separation Science and Technology* 43 (6) 2008: pp. 1382–1403.
<https://doi.org/10.1080/01496390701885331>
 27. **Hao, O.J., Kim, H., Chiang, P.C.** Decolorization of Wastewater *Critical Reviews in Environmental Science and Technology* 30 (4) 2000: pp. 449–505.
<https://doi.org/10.1080/10643380091184237>
 28. **Singh, K.P., Gupta, S., Singh, A.K., Sinha, S.** Optimizing Adsorption of Crystal Violet Dye from Water by Magnetic Nanocomposite Using Response Surface Modeling Approach *Journal of Hazardous Materials* 186 (2–3) 2011: pp. 1462–1473.
<https://doi.org/10.1016/j.jhazmat.2010.12.032>
 29. **Adams, E.** The Antibacterial Action of Crystal Violet *Journal of Pharmacy and Pharmacology* 19 (12) 1967: pp. 821–826.
<https://doi.org/10.1111/j.2042-7158.1967.tb09550.x>
 30. **Gülcemal, S., Çetinkaya, B.** Palladium-EDTA and Palladium-EdteH₄ Catalyzed Heck Coupling Reactions in Pure Water *Turkish Journal of Chemistry* 37 (5) 2013: pp. 40–847.
<https://doi.org/10.3906/kim-1304-12>
 31. **Mani, S., Bharagava, R.N.** Exposure to Crystal Violet, Its Toxic, Genotoxic and Carcinogenic Effects on Environment and Its Degradation and Detoxification for Environmental Safety *Reviews of Environmental Contamination and Toxicology* 237 2016: pp. 71–104.
https://doi.org/10.1007/978-3-319-23573-8_4
 32. **Olam, M., Gündüz, F., Karaca, H.** Production of Activated Carbon from Duckweed and Its Effectiveness in Crystal Violet Adsorption *Biomass Conversion and Biorefinery* 14 2023: pp. 19597–19612.
<https://doi.org/10.1007/s13399-023-04429-w>
 33. **Nizamuddin, S., Baloch, H.A., Griffin, G.J., Mubarak, N.M., Waheed Bhutto, A., Abro, R., Ali Mazari, S., Si Ali, B.** An Overview of Effect of Process Parameters on Hydrothermal Carbonization of Biomass *Renewable and Sustainable Energy Reviews* 73 2017: pp. 1289–1299.
<https://doi.org/10.1016/j.rser.2016.12.122>
 34. **Ahmed, M.B., Hasan Johir, M.A., Zhou, J.L., Hao Ngo, H., Duc Nghiem, L., Richardson, C., Ali Moni, M., Bryant, M.R.** Activated Carbon Preparation from Biomass Feedstock: Clean Production and Carbon Dioxide Adsorption *Journal of Cleaner Production* 225 2019: pp. 405–413.
<https://doi.org/10.1016/j.jclepro.2019.03.342>
 35. **Mohanty, K., Naidu, J.T., Meikap, B.C., Biswas, M.N.** Removal of Crystal Violet from wastewater by Activated Carbons Prepared from Rice Husk *Industrial & Engineering Chemistry Research* 45 (14) 2006: pp. 5165–5171.
<https://doi.org/10.1021/ie060257r>
 36. **Ashour, M., Alprol, A.E., Khedawy, M., Abualnaja, K.M., Mansour, A.T.** Equilibrium and Kinetic Modeling of Crystal Violet Dye Adsorption by a Marine Diatom, *skeletonema costatum* *Materials (Basel)* 15 (18) 2022: pp. 6375.
<https://doi.org/10.3390/ma15186375>
 37. **Khan, M.M., Khan, A., Bhatti, H.N., Zahid, M., Alissa, S.A., El-Badry, Y.A., Hussein, E.E., Iqbal, M.** Composite of polypyrrole with sugarcane Bagasse Cellulosic Biomass and Adsorption Efficiency for 2,4-dichlorophenoxy Acetic Acid in Column Mode *Journal of Materials Research and Technology* 15 2021: pp. 2016–2025.
<https://doi.org/10.1016/j.jmrt.2021.09.028>
 38. **Shafeeyan, M.S., Daud, W., Houshmand, A., Shamiri, A.** A Review on Surface Modification of Activated Carbon for Carbon Dioxide Adsorption *Journal of Analytical and Applied Pyrolysis* 89 (2) 2010: pp. 143–151.
<https://doi.org/10.1016/J.JAAP.2010.07.006>
 39. **Jini, D., Aravind, M., Alsaiari, N.S., Alzahrani, F.M., Sillanpää, M.** Investigation on Structural, Optical, Morphological, Electrical, Mechanical and Biological Activities of Pure and Crystal Violet Dye-Doped Epsomite Single Crystal *Journal of Materials Science: Materials in Electronics* 34 (1) 2023: pp. 61.
<https://doi.org/10.1007/s10854-022-09468-z>
 40. **Nasiri, R., Zarei, M., Arsalani, N., Pezhhanfar, S., Someh, A.A., Panahian, Y.** One-pot Synthesis of Novel 3D Graphene/Fe₃O₄/agro-based Waste Material (Sesamum

- indicum) Nanocomposite for Wastewater Treatment and Artificial Neural Network Modeling *Chemical Engineering Research and Design* 190 2023: pp. 451–463.
<https://doi.org/10.1016/j.cherd.2022.12.044>
41. **Nasiri, R., Arsalani, N.** Synthesis and Application of 3D Graphene Nanocomposite for the Removal of Cationic Dyes from Aqueous Solutions: Response Surface Methodology Design *Journal of Cleaner Production* 190 2018: pp. 63–71.
<https://doi.org/10.1016/j.jclepro.2018.04.143>
 42. **Kheradmand, A., Negarestani, M., Mollahosseini, A., Shayesteh, H., Farimaniraad, H.** Low-cost Treated Lignocellulosic Biomass Waste Supported with FeCl₃/Zn(NO₃)₂ for Water Decolorization *Scientific Reports* 12 (1) 2022: pp. 16442.
<https://doi.org/10.1038/s41598-022-20883-4>
 43. **Fabiyi, J.S., McDonald, A.G., Wolcott, M.P., Griffiths, P.R.** Wood Plastic Composites Weathering: Visual Appearance and Chemical Changes *Polymer Degradation and Stability* 93 (8) 2008: pp. 1405–1414.
<https://doi.org/10.1016/j.polymdegradstab.2008.05.024>
 44. **Guo, D., Li, Y., Cui, B., Hu, M., Luo, M., Ji, B., Liu, Y.** Natural Adsorption of Methylene Blue by Waste Fallen Leaves of Magnoliaceae and Its Repeated Thermal Regeneration for Reuse *Journal of Cleaner Production* 267 2020: pp. 121903.
<https://doi.org/10.1016/j.jclepro.2020.121903>
 45. **George, G., Mahendran, A., Anandhan, S.** Use of Nano-ATH as a Multi-Functional Additive for Poly(Ethylene-co-vinyl Acetate-co-carbon Monoxide) *Polymer Bulletin* 71 (8) 2014: pp. 2081–2102.
<https://doi.org/10.1007/s00289-014-1174-6>
 46. **Asemani, M., Rabbani, A.R.** Detailed FTIR Spectroscopy Characterization of Crude Oil Extracted Asphaltenes: Curve Resolve of Overlapping Bands *Journal of Petroleum Science and Engineering* 185 2020: pp. 106618.
<https://doi.org/10.1016/j.petrol.2019.106618>
 47. **Chen, Y., Zou, C., Mastalerz, M., Hu, S., Gasaway, C., Tao, X.** Applications of Micro-Fourier Transform Infrared Spectroscopy (FTIR) in the Geological Sciences – A Review *International Journal of Molecular Sciences* 16 (12) 2015: pp. 30223–30250.
<https://doi.org/10.3390/IJMS161226227>
 48. **Abdulhameed, A.S., Jawad, A.H., Kashi, E., Radzun, K.A., Alothman, Z.A., Wilson, L.D.** Insight into Adsorption Mechanism, Modeling, and Desirability Function of Crystal Violet and Methylene Blue Dyes by Microalgae: Box-Behnken Design Application *Algal Research* 67 2022: pp. 102864.
<https://doi.org/10.1016/j.algal.2022.102864>
 49. **Essekri, A., Hsini, A., Naciri, Y., Laabd, M., Ajmal, Z., El Ouardi, M., Ait Addi, A., Albourine, A.** Novel Citric acid-functionalized Brown Algae with a High Removal Efficiency of Crystal Violet Dye from Colored Wastewaters: Insights into Equilibrium, Adsorption Mechanism, and Reusability *International Journal of Phytoremediation* 23 (4) 2021: pp. 336–346.
<https://doi.org/10.1080/15226514.2020.1813686>
 50. **Jani, N.A., Haddad, L., Abdulhameed, A.S., Jawad, A.H., Alothman, Z.A., Yaseen, Z.M.** Modeling and Optimization of the Adsorptive Removal of Crystal Violet Dye by Durian (*Durio Zibethinus*) Seeds Powder: Insight into Kinetic, Isotherm, Thermodynamic, and Adsorption Mechanism *Biomass Conversion and Biorefinery* 1 2022: pp. 1–14.
<https://doi.org/10.1007/s13399-022-03319-x>
 51. **Qian, W., Sun, F., Xu, Y., Qiu, L., Liu, C., Wang, S., Yan, F.** Human Hair-derived Carbon Flakes for Electrochemical Supercapacitors *Energy & Environmental Science* 7 (1) 2014: pp. 379–386.
<https://doi.org/10.1039/c3ee43111h>
 52. **Kukulka, W., Wenelska, K., Baca, M., Chen, X., Mijowska, E.** From Hollow to Solid Carbon Spheres: Time-dependent Facile Synthesis *Nanomaterials* 8 (10) 2018: pp. 861.
<https://doi.org/10.3390/nano8100861>
 53. **Priya, M., Mahadevan, C.K.** Preparation and Dielectric Properties of Oxide Added NaCl-KCl Polycrystals *Physica B: Condensed Matter* 403 (1) 2008: pp. 67–74.
<https://doi.org/10.1016/j.physb.2007.08.009>
 54. **Guo, C., Huang, D., Su, Q.** Methods to Improve the Fluorescence Intensity of CaS:Eu²⁺ Red-emitting Phosphor for White LED *Materials Science and Engineering: B* 130 (1–3) 2006: pp. 189–193.
<https://doi.org/10.1016/j.mseb.2006.03.008>
 55. **Yakubu, Y., Zhou, J., Shu, Z., Zhang, Y., Wang, W., Mbululo, Y.** Potential Application of Pre-treated Municipal Solid Waste Incineration Fly Ash as Cement Supplement *Environmental Science and Pollution Research* 25 (16) 2018: pp. 16167–16176.
<https://doi.org/10.1007/s11356-018-1851-3>
 56. **Hariyanto, B., Wardani, D.A.P., Kurniawati, N., Har, N.P., Darmawan, N., Irzaman, I.** X-ray Peak Profile Analysis of Silica by Williamson–Hall and Size-strain Plot Methods *In: Journal of Physics: Conference Series* 2019 2021: pp. 012106.
<https://doi.org/10.1088/1742-6596/2019/1/012106>
 57. **Koochakzadeh, F., Norouzbeigi, R., Shayesteh, H.** Statistically Optimized Sequential Hydrothermal Route for FeTiO₃ Surface Modification: Evaluation of Hazardous Cationic Dyes Adsorptive Removal *Environmental Science and Pollution Research* 30 (7) 2022: pp. 19167–19181.
<https://doi.org/10.1007/s11356-022-23481-z>
 58. **Fan, Y., Liu, W., Kang, Z., Ding, T., Bo, Q., Xiao, L., Bai, X., Zheng, P., Li, Q.** Structural and Electrical Properties of the YSZ/STO/YSZ Heterostructure *Journal of Nanomaterials* 1 2014: pp. 1–5.
<https://doi.org/10.1155/2014/783132>
 59. **Khajonrit, J., Sichumsaeng, T., Kalawa, O., Chaisit, S., Chinnakorn, A., Chanlek, N., Maensiri, S.** Mangosteen Peel-derived Activated Carbon for Supercapacitors *Progress in Natural Science: Materials International* 32 (5) 2022: pp. 570–578.
<https://doi.org/10.1016/j.pnsc.2022.09.004>
 60. **Gao, Y., Yue, Q., Gao, B., Li, A.** Insight into Activated Carbon from Different Kinds of Chemical Activating Agents: A Review *Science of The Total Environment* 746 2020: pp. 141094.
<https://doi.org/10.1016/j.scitotenv.2020.141094>
 61. **Zhang, N., Shen, Y.** One-step Pyrolysis of Lignin and Polyvinyl Chloride for Synthesis of Porous Carbon and its Application for Toluene Sorption *Bioresource Technology* 284 2019: pp. 325–332.
<https://doi.org/10.1016/j.biortech.2019.03.149>
 62. **Olam, M.** Determination of the Effectiveness of Carbons Obtained from the Co-carbonization of Duckweed and Waste Coffee on Crystal Violet Removal *Bitlis Eren Üniversitesi Fen Bilimleri Dergisi* 12 (1) 2023: pp. 207–214.
<https://doi.org/10.17798/BITLISFEN.1223614>
 63. **Foroutan, R., Peighambardoust, S.J., Peighambardoust, S.H., Pateiro, M., Lorenzo, J.M.**

- Adsorption of Crystal Violet Dye Using Activated Carbon of Lemon Wood and Activated Carbon/Fe₃O₄ Magnetic Nanocomposite from Aqueous Solutions: A kinetic, Equilibrium and Thermodynamic Study *Molecules* 26 (8) 2021: pp. 2241.
<https://doi.org/10.3390/molecules26082241>
64. **Sabna, V., Thampi, S.G., Chandrakaran, S.** Adsorption of Crystal Violet onto Functionalised Multi-walled Carbon Nanotubes: Equilibrium and Kinetic Studies *Ecotoxicology and Environmental Safety* 134 2016: pp. 390–397.
<https://doi.org/10.1016/J.ECOENV.2015.09.018>
65. **AL-Shehri, H.S., Almudaifer, E., Alorabi, A.Q., Alanazi, H.S., Alkorbi, A.S., Alharthi, F.A.** Effective adsorption of Crystal Violet from Aqueous Solutions with Effective Adsorbent: Equilibrium, Mechanism Studies and Modeling Analysis *Environmental Pollutants and Bioavailability* 33 (1) 2021: pp. 214–226.
<https://doi.org/10.1080/26395940.2021.1960199>
66. **Yusuff, A.S., Ajayi, O.A., Popoola, L.T.** Application of Taguchi Design Approach to Parametric Optimization of Adsorption of Crystal Violet Dye by Activated Carbon from Poultry Litter *Scientific African* 13 2021: pp. e00850.
<https://doi.org/10.1016/j.sciaf.2021.e00850>
67. **Olam, M.** Co-carbonization of Hazelnut Shell and Lemna minor: Its Effectiveness in Adsorption of Crystal Violet from an Aqueous Solution *Separation Science and Technology* 59 (5) 2024: pp. 737–747.
<https://doi.org/10.1080/01496395.2024.2349177>
68. **Muthukumar, C., Sivakumar, V.M., Thirumarimurugan, M.** Adsorption Isotherms and Kinetic Studies of Crystal Violet Dye Removal from Aqueous Solution Using Surfactant Modified Magnetic Nanoadsorbent *Journal of the Taiwan Institute of Chemical Engineers* 63 2016: pp. 354–362.
<https://doi.org/10.1016/j.jtice.2016.03.034>



© Olam. 2024 Open Access This article is distributed under the terms of the Creative Commons Attribution 4.0 International License (<http://creativecommons.org/licenses/by/4.0/>), which permits unrestricted use, distribution, and reproduction in any medium, provided you give appropriate credit to the original author(s) and the source, provide a link to the Creative Commons license, and indicate if changes were made.